Article:
Salembier, C, Villeirs, G, De Bari, B et al. (2 more authors) (2018) ESTRO ACROP consensus guideline on CT- and MRI-based target volume delineation for primary radiation therapy of localized prostate cancer. Radiotherapy and Oncology, 127 (1). pp. 49-61. ISSN 0167-8140

https://doi.org/10.1016/j.radonc.2018.01.014

ESTRO-ACROP consensus guideline on CT- and MRI-based target volume delineation for primary radiation therapy of prostate cancer

Carl Salembier[1], Geert Villeirs[2], Berardino De Bari[3], Peter Hoskin[4], Bradley Pieters[5], Marco Van Vulpen[6], Vincent Khoo[7], Ann Henry[8], Alberto Bossi[9], Gert De Meerleer[10], Claus Belka[11], Valérie Fonteyne[12*]

1. Department of Radiotherapy, Europe Hospitals Brussels, Belgium
2. Department of Radiology, Ghent University Hospital, Belgium
3. Radiation Oncology, Centre Hospitalier Universitaire Vaudois (CHUV), Lausanne, Switzerland
4. Cancer centre, Mount Vernon Cancer Centre, Northwood, United Kingdom
5. Department of Radiation Oncology, Academic Medical Center, Amsterdam, The Netherlands
6. Department of Radiation-Oncology, University Medical Center Utrecht, The Netherlands
7. Department of Clinical Oncology, Royal Marsden Hospital, London, United Kingdom
8. Leeds Cancer Centre, Leeds Teaching Hospitals NHS Trust, Leeds, United Kingdom
9. Department of Radiation Oncology, Institut Gustave Roussy, Villejuif, France
10. Department of Radiation Oncology, University Hospital Leuven, Belgium
11. Department of Radiation Oncology, University of Munich, München, Germany
12. Department of Radiotherapy, Ghent University Hospital, Belgium

Abstract

Background and purpose

Delineation of clinical target volumes (CTVs) remains a weak link in radiation therapy (RT), and large inter-observer variation is seen. Guidelines for target and organs at risk delineation for prostate cancer in the primary setting are scarce. The aim was to develop a delineation guideline obtained by consensus between a broad European group of radiation oncologists.

Material and methods

During ESTRO teaching courses on prostate cancer, teachers sought consensus on delineation of CTV through dialogue and based on cases. One teacher delineated a CTV prostate, seminal vesicles and rectum on co-registered CT and MRI scans. All participants were asked to contour the case via a web-based platform. Results were communicated and were followed by discussion, adaptation of the delineation and formulation of these guidelines.

Results

The study confirmed a large inter-observer variation despite incorporating prostate MR imaging, and confirm the need for clear delineation guidelines and additional clinician training.

Conclusion

The ESTRO-ACROP consensus on CT/MRI based CTV delineation for primary RT of prostate cancer, endorsed by a broad base of the radiation oncology community, is presented to improve consistency.

Keywords

prostate cancer; CTV prostate, seminal vesicles, rectum, primary radiation therapy; CT-based delineation; MRI-based delineation

Introduction

Over the past decades, high-dose external beam radiotherapy (EBRT) and image-guided radiotherapy (IGRT) have been implemented in the treatment of prostate cancer (PC) patients worldwide. With modern radiation techniques sharp dose gradients are created. This results in the delivery of very high doses to the prostate while sparing the surrounding tissues. To avoid underdosages, a proper definition and accurate contouring of the target volume are mandatory. For postoperative radiotherapy, contouring guidelines have been developed to facilitate the delineation of the postoperative prostate bed (1-5). For primary PC, in contrast, contouring guidelines are scarce. In 2006, the European Organisation for Research and Treatment of Cancer (EORTC) group formulated CT-based prostate contouring guidelines (6). Despite these guidelines a large inter-observer variability in the delineation of the clinical target volume (CTV) of PC patients has been reported (7-8).

With Magnetic Resonance Imaging (MRI), multiplanar image series are acquired. This, combined with high soft-tissue contrast on T2-weighted images results in a detailed visualisation of the prostate and periprostatic structures. It has been shown that the addition of MRI to CT results in a decrease in inter-observer contouring variation and smaller prostate volumes (9-11).

The first aim of this analysis is to describe the variations in CT and MRI-based CTV contouring of the prostate performed by physicians with large experience in EBRT for PC. Subsequently, consensus guidelines for CTV delineation of the prostate with and without MRI, derived from these observations, are proposed.

Material and methods

Nine radiation-oncologists and one radiologist (GV), all experienced in PC treatment, were asked to delineate as Regions of Interest (ROIs) the rectum, the CTV of the prostate and seminal vesicles (SV) separately. The rectum was contoured on CT-images only. The prostate was delineated on CT and MRI-images separately. The MRI images were at the disposal of the experts at the time of CT prostate contouring. Matched CT and MRI-images were provided. The CT-scan was obtained with a slice thickness of 2 mm and MRI-scan with a slice thickness of 4 mm.

Patient case

The prostate case was that of 58 years old patient presenting with a PSA of 12 ng/ml. Rectal examination demonstrated a benign feeling prostate. The MRI did not reveal any abnormality. Staging was thus cT1c N0 M0. Random biopsies of the prostate were positive in 2 cylinders out of 6, Gleason score 3+4 at the left side and 1 cylinder out of 6, Gleason score 3+3 at the right side of the prostate.

Tools

For this study, the FALCON platform (Fellowship in Anatomic deLineation and CONtouring) from ESTRO (European SocieTy for Radiotherapy and Oncology) and the software EduCase™ from RadOnc eLearning Center, Inc. Fremont, CA, USA was used. This is a web-based contouring and analysis tool that has a graphical user interface for the management, storage and publishing of contouring of the clinical cases. The software allows image fusion of the simulation CT scan with MRI, as well as an integrated analysis on contouring proficiency. EduCase contour similarity metric tools allows computing metrics

that score a participant contour relative to the reference contour. For evaluation, the participants' contours were tested against the original DICOM structures. EduCase similarity metric includes an Area Domain metric and statistics expressed as areas in units of square centimetres. For each case the contour from the experts is called the Area of Consensus (AC) whereas the contour from a participant is called the Delineated Area (DA). The Area of Intersection (AI) refers to the area of overlap between the AC and DA. The consistency in contouring between expert and participant (AI) as well as areas of non-consistency can be shown on a graphical basis using this software.

Statistical evaluation

All the delineations of the relevant ROIs were used for evaluation. The EduCase software counts the voxels in each reconstruction plane that contained both the reference contours and participant contours for a selected structure providing a calculated DICE index (DI) defined as (12).

$$DI= 2 \times AI/(AC+DA)$$

For the target volumes, i.e. CTV of the prostate and SV, the contours of a radiation oncologist (CS) were used as reference images. For the rectum the contours of the radiologist were set as reference images. The set of reference images was not similar for targets and organ at risk. It was agreed on that the contouring of CTV of the prostate and SV differed between radiation-oncologist, taking into account the oncological microscopic spread when contouring the clinical target volume, and radiologist, mainly focusing on anatomical barriers. In contrast it was presumed that the radiologist most accurately delineated the contours of the rectum.

Delineation guidelines

Based on the results of this study we formulated guidelines for the delineation of the rectum, as well as CTV of the prostate and SV.

Results

1. Evaluation of the delineation of the rectum.

The radiologist delineated the reference rectum contour (see above). The average DICE index for the rectum is 0,87 with individual differences ranging form 0,79 to 0,92. All participants started delineation at the same slice number (recto-sigmoid junction). Two participants ended the delineation earlier than the reference and the others at the inferior (anal) level. One participant ended two slices higher and one five slices higher than the last reference slice. Most variations were found at the level of the lower part of the rectum where it is difficult to discriminate the rectum from the posterior border of the prostate and levator ani muscle laterally, although some variation is also seen at the superior level. Detailed information on the calculated DICE indexes for the rectum contour can be found in the additional electronic appendix.

2. Guidelines for CT-based delineation of the rectum with and without MRI (figure 1)

The delineation of the rectum starts at the recto-sigmoid junction, i.e. where the sigmoid colon becomes the rectum, and which usually takes the form of an acute angle.
The rectum contouring ends approximately 2 centimeters below the lowest prostate-apex contour.
For rectum delineation following guidelines can be applied:

1) In the axial plane: delineate the rectum contour on all slices where it can be differentiated from the surrounding tissues, i.e. prostate, anal sphincter and levator ani muscle.
2) In the mid-sagittal plane:
    a. visualize all rectum contours that were delineated in the axial planes

b. create a ‘contouring help-structure’ by connecting the anterior and posterior borders of the projected rectum slices

3) In the axial plane: display the ‘contouring help-structure’. Based on this ‘contouring help-structure’ one can add missing rectum slices and adjust where necessary to the formerly delineated rectum contour.
4) In the sagittal plane: project the final rectum contour as a control for detecting inappropriate protrusions of the rectum. If present adjust in the axial plane.

Added value of MRI:

The prostate is surrounded by a prostatic capsule that is a thin and firmly adherent non-glandular fibromuscular band. On T2-weighted MR-images the prostatic capsule is usually visible as a sharply demarcated dark rim. This is most easily visualized at the posterolateral borders of the prostate. With MRI, a better discrimination between the posterior border of the prostate and the anterior rectal wall is thus obtained when compared to CT images only. When a fixed protocol is present for rectal emptying, which is applied equally before both CT and MRI examinations, the rectal contour on MRI can help in the definitive delineation of the rectum on CT in case of doubt.

3. Evaluation of the CTV prostate and SV contours

The reference contours of the CTV prostate as well of the SV contours were defined by one radiation oncologist (CS) (see above). The evaluation on contouring was first done with the whole prostate, and thereafter the three sub-regions (base-region, mid-prostate-region and apex-region) were analysed.

3.1 Evaluation of the CTV prostate on CT-scan:

The average DICE index for the whole prostate was 0.84 compared to the reference contours, with individual differences ranging from 0.77 to 0.90. Looking at the described sub-regions of the prostate, the mid-prostate delineation showed high DICE indices for the majority of the participants, with a mean of 0,88 with individuals ranging from 0,78 to 0,93. On the contrary, the delineation of the base and the apex showed a high inter-observer variability. The DICE indices at the base of the prostate had a mean of 0,82 with individuals ranging from 0,66 to 0,94. At the apex of the prostate the mean DICE index was only 0,69 with individuals ranging from 0,50 to 0,83. More detailed information can be found in the electronic appendix.

3.2 Evaluation of the CTV prostate on MRI-scan:

As for the evaluation on CT-scan, the evaluation on MRI-scan was first done with the whole prostate, and thereafter, the three sub-regions (base-region, mid-prostate-region and apex-region) were analysed. The average DICE index for the whole prostate was 0.75 compared to the reference contours, with individual differences ranging from 0.51 to 0.85. Surprisingly this is worse than for CT based delineation. Looking at the described sub-regions of the prostate, the mid-prostate delineation showed high DICE indices for the majority of the participants, with a mean of 0,88, however with individuals ranging from 0,68 to 0,93. Two participants missed slices on the inferior border of the mid-prostate or contoured only the central lobe explaining the huge individual ranging. On the contrary, the delineation of the base and the apex showed a very high inter-observer variability amongst almost all participants. The DICE indices at the base of the prostate had a mean of 0,71 with individuals ranging from 0,54 to 0,86. At the apex of the prostate the mean DICE index was only 0,51

with individuals ranging from 0,0 to 0,74. More detailed information can be found in the electronic appendix.

3.3 Evaluation of the SV contours on CT-scan:

The average DICE index for the seminal vesicles was 0.76 compared to the reference contours, with individual differences ranging from 0.58 to 0.85. More detailed information can be found in the electronic appendix.

3.4 Evaluation of the SV contours on MRI-scan:

The average DICE index for the seminal vesicles was 0.73 compared to the reference contours, with individual differences ranging from 0.55 to 0.86. The major difference with the delineation on CT-scan is that there was a larger variation in starting and ending slice for this delineation. More detailed information can be found in the electronic appendix.

4. Guidelines for CT-based delineation of the CTV of the prostate with and without MRI (Table 1 and Figure 2).

1) Defining the level of the apex (figure 2A-D):

   The apex of the prostate is the lowermost portion of the "inverted pyramid" that constitutes the prostate. The exact caudal extent of the apical glandular elements is often difficult to assess, because they are interspersed among fibromuscular tissue of the pelvic floor.

   As described by McLaughlin et al (13), a lateral-view inspection from the prostate and genito-urinary diaphragm (GUD) elements can be useful to define the prostate apex.

Following the description of McLaughlin et al, three separate levels can be defined above the penile bulb (figure 2A). First, a triangle-shaped sling, spanning the pelvic bones as opposed to the penile bulb level, can be visualised on CT immediately above the penile bulb. There, a distinct plane of separation is apparent between the central penile bulb and the muscle attached to the pelvic bones. Above this triangle level a circular-shaped region resulting from the external sphincter passing through the GUD (figure 2B) can be recognized. This may be visible on CT as a central circular area. Third, a hourglass or slit shape that results from the in-bowing of the levator ani just below the apex can sometimes be recognized on CT. On CT, the apex of the prostate appears to merge completely with the levator ani. Consequenlty, a continuous and homogeneous density extending from side to side without a visible circle or slit defines the apex level on CT (figure 2C). Mc Laughlin concludes that, if one begins at the penile bulb level and proceeds superiorly on CT to define the triangle, circle, and slit/hourglass if visible and calls the first CT slice without recognizable GUD elements the apex, it is possible to avoid gross overestimation resulting from inclusion of obvious GUD elements (13).

Whenever visible, the urethra should be excluded from the apex, creating a butterfly shaped structure, except in cases where urethral involvement is suspected.

Added value of MRI:

The apex of the prostate is usually recognized as a bilateral triangular area of high T2-signal intensity peripheral zone tissue that contrasts well with the caudal urogenital diaphragm and the lateral levator ani muscle. It also contrasts well with the low signal intensity prostatic sphincter (Figure 2D). The major advantage of implementing MRI

for apical delineation is that it enables a better approximation of the caudal aspect of the apex. Furthermore, the external sphincter and distal urethra can be safely excluded from the target volume, because it contrasts well with the apical glandular tissue.

2) Defining the lateral borders of the prostate (figure 2E-F):

The levator ani muscles support the prostate. The prostate does not extend into or beyond the levator ani muscles, except for a clinical (c)T4 PC, which is rarely missed on digital rectal examination. The levator ani muscle thus confines the inferolateral border of the prostate and should not be included in the prostate contour, except in case of suspicion of cT4 PC. The levator ani muscles are usually thicker anteriorly (next to the prostate) than posteriorly (next to the rectum), especially at the apical level (so-called 'levator prostatae'). However, in the absence of MRI, no discrimination can be made based on CT images only between the levator ani muscles and the prostate. Therefore we advise to assume that the levator ani muscles next to the prostate will have the same (thinner) thickness as next to the rectum. By doing so, a potential under dosage of the prostate is avoided at the cost of some excess muscle irradiation.

Added value of MRI:

On T2-weighted MR-images the levator ani muscles have low signal intensity in contrast with the high signal intensity of the normal peripheral zone tissue of the prostate, markedly improving the discrimination between both tissues. This is of importance, as, as mentioned previously, the levator ani muscles are the thickest at the lower part of the prostate and external urethral sphincter. The levator ani muscles become thinner at the upper half of the prostate where their thickness is comparable to the thickness of the levator ani muscles flanking the rectum. Consequently

implementing MRI for prostate delineation results in a more accurate contouring of the lateral borders of the prostate, most importantly at the level of the apex, and univocally leads to smaller target volumes as unnecessary inclusion of the levator ani muscles is avoided.

3) Defining the anterior border of the prostate (figure 2G-H):

The retropubic space or 'Retzius' space is located anterior to the prostate and contains fatty tissue and Santorini's venous plexus (figure H). Anteriorly, the prostate is covered with the prostatic fascia. The anterior surface of the prostate itself consists of the anterior fibromuscular stroma (AFMS) that is composed of fibrous and smooth muscular elements. On CT, it is usually difficult to locate the anterior extent of the AFMS due to the adjacent venous plexus with similar density. As a consequence, the anterior prostate contour is difficult to delineate on CT, with frequent inclusion of the venous plexus. Furthermore, as up to 25% of the PCs are located in the transition zone (14) and can invade the AFMS, the exact anterior extension of the tumor is difficult to assess. In the absence of MRI, we therefore suggest to include in the prostate contour all non-fatty tissue in the posterior Retzius' space.

Added value of MRI:

On T2-weighted MR-images, the AFMS of the prostate, which contains no glandular elements, has low signal intensity and forms as such a clear barrier to the high signal intensity Santorini's venous plexus (due to slow-flowing venous blood) and the equally high signal intensity adipose tissue in Retzius' space. Implementing T2-weighted MR-information for prostate delineation hence prevents the unnecessary inclusion of mainly vascular structures resulting in an increased target volume.

4) Defining the posterior border of the mid-prostate:

The posteriorly located Denonvilliers' fascia of the prostate represents an effective barrier for tumor spread into the rectum. Wherever there is no clear fat plane demarcating the prostate from the rectum, the posterior border of the prostate should be contoured adjacent to the anterior rectal wall (see above).

Added value of MRI:

As mentioned previously, the prostatic capsule is usually visible as a sharply demarcated dark rim on T2-weighted MR-images, best recognizable at the level of the posterolateral border of the prostate. Furthermore, the dark signal intensity of the rectum contrasts well with the high signal intensity of the normal prostatic peripheral zone. With MRI, therefore, a better discrimination between the posterior border of the prostate and the anterior rectal wall when compared to CT images only is expected.

5) Defining the base of the prostate:

The base of the prostate is in continuity with the bladder. Ideally, 100 cc of intravenous contrast is administered 10 minutes prior to scanning in a well-hydrated patient. The advantage of using intravenous contrast preparation before CT scanning is the unequivocal distinction between the base of the prostate and the bladder lumen (figure 2I). Also protrusion of the prostate into the bladder due to benign prostate hypertrophy can be taken into account. We therefore recommend the routine use of contrast on planning-CT, unless contra-indicated.

Added value of MRI

Protrusion of prostatic hyperplasia into the bladder base can be easily visualized on T2-weighted MRI and add to a correct delineation of the prostate especially when no contrast was administered prior to CT.

6) Defining the seminal vesicles

The SV can be omitted from the target volume in low risk PC patients (pre-treatment characteristics: PSA ≤10 ng/ml; biopsy Gleason score ≤6 and clinical stage ≤T2a; ≤50% of positive biopsies) (15). For intermediate (PSA>10 and ≤20 ng/ml or Gleason score of 7 or clinical stage T2b) and high risk (PSA>20 ng/ml or Gleason score of >7 or clinical stage >T2b) PC patients the SV should be included. Based on surgical series and the publication of Qi et al, we propose to include the proximal 1.4 cm and 2.2 cm of SV delineated in the axial plane for intermediate and high risk PC patients respectively (16). The most proximal part of the SV (starting point) is the point where the SV appears individually (i.e. separated from the prostatic base) on the most caudal transverse plane that depicts the SV. The vas deferent ducts, consisting of a thin tubular structure that can be recognized cranial and medial to each SV, should not be included in this delineation (Figure 2J).

Added value of MRI

The SV are grapelike pouches filled with fluid, and have high signal intensity on T2-weighted MR-images. They are located caudo-lateral to the vas deferent ducts, which are easily distinguishable from the SV and from surrounding vascular structures due to their low signal intensity. Hence they can be safely omitted from the target volume. Abnormal mass-like low signal intensity in the SV is suggestive for seminal vesicle invasion. If the latter is present, the entire SV should be included in the target volume,

despite tumor characteristics. As such, information from the MRI also allows evaluation to what extent the SV should be included. On the other hand, absence of signs suggestive for SV invasion should not alter the decision to include the SV, which remains a decision that is based on tumor characteristics, i.e. PSA, Gleason score and T-stage (15).

7) How to compensate for potential ECE?

The risk of ECE is limited for patients with low risk PC (PSA ≤10 ng/ml; biopsy Gleason score ≤6 and clinical stage ≤T2a and <50% of the biopsies involved) (15). With higher PSA level and Gleason score, not only the risk of ECE, but also the extent of ECE increases. Based on the results of Chao et al and Teh et al, we advise to expand the prostate contour (without seminal vesicles) with 2.5 mm and 5 mm for patients with intermediate (PSA>10 and ≤20 ng/ml or Gleason score of 7 or clinical stage T2b) and high risk PC (PSA >20 ng/ml or Gleason score ≥8 or clinical stage ≥T2c) respectively, if CT is the only imaging modality (17-18).

Added value of MRI

On MRI, capsular perforation can be suspected in the presence of clear signs of ECE, such as an irregular margin, periprostatic fat infiltration, obliteration of the rectoprostatic angle or measurable tumor in the periprostatic fat. If ECE is suspected on MRI the area of ECE should always be included in the prostate contour. Only when the probability of ECE on MRI is very low, i.e. a suspicious intraprostatic lesion **without** capsular contact, no additional margins are required, however, the experience of the radiologist and quality of the MR examination have to be taken into account. In

case of doubt the above-mentioned recommendations for target expansion need to be applied.

8) Review in the sagittal and coronal view

Review and control of the prostate contour in the sagittal and coronal view is necessary to detect discrepancies in the prostate contouring and allow adjusting where necessary (8).

5. Practical considerations when delineating the prostate on CT and MRI (Figure 6).

1) MRI quality requirements

Clinical guidelines for multiparametric MRI are provided in the prostate imaging reporting and data system version 2 (PI-RADS v2) (19).

2) When performing a MRI of the prostate for prostate contouring purposes, ideally both MRI and CT are performed in similar conditions, i.e. applying the same protocol for bladder filling and emptying of the rectum (i.e. use of fleet enema) as well as treatment position (i.e. recommended to use a flat table, knee-fix, ankle-fix). Even in the absence of an automatic fusion modality for online fused contouring, MRI images can be used for off-line co-registration with the planning CT images. Differences in slice thickness of MRI and CT images have to be taken into account.

3) Prior to the delineation of the prostate contour both image sets have to be aligned. This alignment can be based on bony structures, for example closure of the pubic bones, combined with vascular structures lying in the peri-prostatic fat. Once both image sets are aligned the prostate contours of the MRI images can be extrapolated to the CT images.

Discussion

With modern radiation techniques, enabling us to create very sharp dose gradients, errors in the delineation of the target volume have, more then ever, a direct impact on treatment outcome. For instance, tumour control can decrease due to an underdosage of the prostate. The risk of toxicity, on the other hand, is increased due to the unintended inclusion of surrounding tissues in the high dose region (20). In this study, 9 physicians, experienced in PC treatment, were asked to delineate the CTV of the prostate, both on CT and MRI, according to the protocol used at their institution. Based on the observed inconsistencies in our analysis, we propose detailed guidelines for future delineation of the CTV of the prostate and rectum.

A large variability in CT-based prostate contouring has been reported, despite existing guidelines (21-22). These inconsistencies are attributed to poor soft tissue contrast between the prostate, rectum and pelvic floor muscles on CT. Gao et al, reported that a CT based delineated prostate volume is on average 30% larger than the true prostate volume defined on photographic anatomical images from the visible human project. Nevertheless, only 84% of the true prostate volume appears to be included in this contoured target volume (21). The posterior parts of the prostate are most often missed while there is a tendency to overextend the anterior border (21).

Prostate contouring can be improved by gaining better insights in the normal anatomy of the male pelvis (14). Also education programs have shown to reduce both the inter-and intra-observer variability (23-24) of the prostate delineation with 15% and 9% respectively on CT (23).

MRI is currently the best modality to depict the anatomy of the prostate, as it enables a more detailed discrimination between the prostate and periprostatic tissue. Consequently, the implementation of MRI in prostate delineation leads to a significant reduction in both prostate

volume and interobserver variability compared to CT based only delineation (11, 25). The largest benefit of MRI is observed at the level of the apex of the prostate (26). Our study confirms important discrepancies found in the delineation of the apex, however this remained present even with additional MRI-information. The low consistency in apex delineation observed in our study is attributed to differences in in- or exclusion of the distal part of urethra from the prostate contour. This suggests that, besides implementing better imaging, a clear definition of the prostate target volume is needed in the era of modern radiation techniques. Since the distal part of the urethra within the external sphincter is seldom invaded, we recommend to omit this part of the urethra unless invasion is suspected on MRI, creating a butterfly shaped contour excluding the urethra at the level of the apex.

As pointed out by others and confirmed in our study, large variations are also seen in the delineation of the SV. Again, lack of clear guidelines on when and how to delineate the SV contribute to these findings.

With MRI a maximum sensitivity and specificity of 82% for the detection of SV invasion is reported (27). The ultimate decision whether or not to include the SV is therefore based on clinical features predicting for SV invasion, rather than MRI. Pathological analysis of radical prostatectomy specimens revealed that SV involvement is most often restricted to the proximal part of the SV. Consequently, the EORTC guidelines recommend including the SV for a length of 1 cm and 2 cm for intermediate and high-risk PC respectively (6). Qi et al, compared the actual anatomic volume of the SV with the volume of the SV included in the clinical target volume defined by EORTC and RTOG0815 PC radiotherapy guidelines (16). Based on their observations, they concluded that the current EORTC guidelines inadequately include the proximal 1 cm and 2 cm of SV. They proposed to extent the delineation to the proximal 1.4 cm and 2.2 cm of SV in the axial plane for intermediate and high risk PC patients respectively (16). These recommendations were implemented in the current

guidelines.

Another point of concern is how to deal with ECE. Several nomograms predicting the risk of ECE have been proposed and validated. Also, with higher PSA level and Gleason score, not only the risk of ECE, but also the ECE linear distance increases. Based on radical prostatectomy specimens (17-18) expansion of the prostate contour with 2.5 mm and 5 mm are recommended for patients with intermediate and high risk PC respectively, if CT is the only imaging modality for contouring (6). With a reported positive predictive value for ECE of 87%, MRI allows to accurately evaluate the presence of ECE (27). Blind and large expansions of the target volume, in order to compensate for potential ECE, can thus be avoided if information of MRI is available. However, the experiences of the radiologist as well as the quality of the MR examination have to be taken into account.

Studies have shown that local failure mainly occurs at the level of the initial dominant intraprostatic lesion (28-29). Therefore, there is growing interest in escalating the dose focally to the area that is at highest risk of local failure. Several studies have examined the place of PET-CT for delineation of the prostate and /or intraprostatic lesion (30-31). The reported data are however not conclusive. Considering the low sensitivity and specificity of PET-CT in the detection of primary prostate cancer, its routine use for target delineation cannot be recommended (30-31).

Multiparametric MRI in contrast is frequently used for the visualisation of such dominant intraprostatic lesions. A recent meta analysis showed that mpMRI is able to detect significant PCa with a sensitivity range of 44% to 87% and a negative predictive value range of 63% to 98% (32). Models, which accurately incorporate the information of MRI in the treatment planning with a focal boost on the dominant intraprostatic lesion, have been published in the meanwhile (33). However whether or not the performance of a focal boost to the dominant intraprostatic lesion is beneficial still has to be proven. This is currently evaluated in an on-

going phase 3 trial randomising intermediate and high-risk PC patients to receive either 77 Gy (35 fractions) to the prostate or 77 Gy to the prostate with an additional boost to the macroscopic tumor up to 95 Gy (34). Until the results of this trial clearly demonstrate the safety and the superiority of this approach, the routine use of focal boost to the dominant intraprostatic lesion cannot be advocated outside clinical trials. Therefore no recommendations were made in these guidelines on how to delineate the dominant intraprostatic lesion.

Considering the advantages of MRI in prostate visualisation, the use of MRI in radiotherapy is rapidly growing. MRI has also already been implemented in the development and integration of a planning, treatment and delivery strategy that is solely based on MRI images (35).

Conclusion

Guidelines to facilitate the delineation of the CTV of the prostate in the primary setting are scarce resulting in an important variation in CTV delineation. This was again demonstrated in our study. New contouring guidelines adapted to modern radiation therapy techniques and including modern imaging are proposed in this manuscript.

References

1. Poortmans, P., Bossi, A., Vandeputte, K. et al, Guidelines for target definition in post-operative radiotherapy for prostate cancer, on behalf of the EORTC Radiation Therapy Oncology Group. Radiotherapy Oncol. 2007;84:121–127.
2. Sidhom, M.A., Kneebone, A.B., Lehman, M. et al, Post-prostatectomy radiation therapy consensus guidelines of the Australian and New Zealand Radiation Oncology Genito-Urinary Goup. Radiotherapy Oncol. 2008;88:10–19.
3. Wiltshire, K.L., Brock, K.K., Haider, M.A. et al, Anatomical boundaries of the clinical target volume (prostate bed) after radical prostatectomy. Int J Radiat Biol Oncol Phys. 2007;69:1090–1099.
4. Michalski, J.M., Lawton, C., Naqa, E. et al, Development of RTOG consensus guidelines for the definition of clinical target volume for postoperative conformal radiation therapy for prostate cancer. Int J Radiat Oncol Biol Phys. 2010;76:361–368.
5. Ost P, De Meerleer G, Vercauteren T, et al. Delineation of the postprostatectomy prostate bed using computed tomography: interobserver variability following the EORTC delineation guidelines. Int J Radiat Oncol Biol Phys. 2011 Nov 1;81(3):e143-9. doi: 10.1016/j.ijrobp.2010.12.057.
6. Boehmer D, Maignon P, Poortmans P, et al. Guidelines for primary radiotherapy of patients with prostate cancer. Radiot Oncol 2006; 259-269.
7. Nakamura K, Shioyama Y, Tokumaru S, et al. Variation of clinical target volume definition among Japanese radiation oncologists in external beam radiotherapy for prostate cancer. Jpn J Clin Oncol 2008; 38: 275-280.
8. Moeckli R, Sozzi W, Mirimanoff R, et al. Physical considerations on discrepancies in target volume delineation. Z Med Phys 2009; 19: 224-235.

9. Rasch C, Barillot I, Remeijer P, et al. Defintion of the prostate in CT and MRI: a multi-observer study. Int J Radiat Oncol Biol Phys 1999; 43: 57-66.
10. Sander L, Langkilde N, Holmberg M and Carl J. MRI target delineation may reduce long-term toxicity after prostate radiotherapy. Acta Oncologica 2014; 53: 809-814.
11. Hentschel B, Oehler W, Straus D, et al. CT-MRI image fusion in IMRT planning for prostate cancer. Strahlenther und Onkol 2011; 187: 183-190.
12. Dice LJ. Measures of the amount of ecologic association between species. Ecology 1945; 26: 297–302.
13. McLaughlin P, Evans C, Feng M and Narayana V. Radiographic and anatomic basis for prostate contouring errors and methods to improve prostate contouring accuracy. Int J Radiat Oncol Biol Phys 2010; 76: 369-378.
14. McNeal J. Normal anatomy of the prostate and changes in benign prostatic hypertrophy and carcinoma. Semin Ultrasound CT MR 1988; 9 (5): 329-334.
15. Lieberfarb ME, Schultz D, Whittington R, et al. Using PSA, biopsy, Gleason score, clinical stage, and the percentage of positive biopsies to identify optimal candidates for prostate-only radiation therapy. Int J Radiat Oncol Biol Phys 2002; 53: 898-903.
16. Qi X, Asaumi J, Zhang M, et al. Optimal contouring of seminal vesicle for definitive radiotherapy of localized prostate cancer: comparison between EORTC prostate cancer radiotherapy guideline, RTOG0815 protocol and actual anatomy. Radiation Oncol 2014; 9: 288-295.
17. Chao K, Goldstein N, Yan D, et al. Clinicopathologic analysis of extracapsular extension in prostate cancer: should the clinical target volume be expanded posterolaterally to,account for microscopic extension? Int J Radiat Oncol Biol Phys 2006; 4: 999-1007.

18. Teh B, Bastasch M, Wheeler T, et al. IMRT for prostate cancer: defining target volume based on correlated pathologic volume disease. Int J Radiat Oncol Biol Phys 2003; 56: 184-191.

19. Barentsz JO, Weinreb JC, Verma S, et al. Synopsis of the PI-RADS v2 Guidelines for Multiparametric Prostate Magnetic Resonance Imaging and Recommendations for Use. Eur Urol 2016; 69: 16-40.

20. Sander L, Langkilde N, Holmberg M and Carl J. MRI target delineation may reduce long-term toxicity after prostate radiotherapy. Acta Oncologica 2014; 53: 809-814.

21. Gao Z, Wilkins D, Eapen L, et al. A study of prostate delineation referenced against a gold standard created from the visible human data. Radiother Oncol 2007; 85: 239-246.

22. Fiorino C, Reni M, Bolognesi A, Cattaneo GM, Calandrino R. Intra- and inter-observer variability in contouring prostate and seminal vesicles: Implications for conformal treatment planning. Radiother Oncol 1998; 47: 285 – 92.

23. Khoo E; Schick K; Plank A, et al. Prostate contouring variation: can it be fixed? Int J Radiat Oncol Biol Phys 2012; 82: 1923-1929.

24. Szumacher E, Harnett N, Warner S, et al. Effectiveness of educational intervention on the congruence of prostate and rectal contouring as compared with a gold standard in three-dimensional radiotherapy for prostate. Int J Radiat Oncol Biol Phys 2010; 76: 379-385.

25. Doemer A, Chetty I, Glide-Hurst C, et al. Evaluating organ delineation, dose calculation and daily localization in an open-MRI simulation workflow for prostate cancer patients. Radiation Oncol 2015; 10: 37-46.

26. Debois M, Oyen R, Maes F, et al. The contribution of magnetic resonance imaging to the three-dimensional treatment planning of localized prostate cancer. Int J Radiat Oncol Biol Phys 1999; 45: 857-865.

27. Engelbrecht MR, Puech P, Colin P, Akin O, Lemaître L and Villers A. Multimodality magnetic resonance imaging of prostate cancer. J Endourol 2010; 24: 677-684.

28. Pucar D, Hricak H, Shukla-Dave A, Kuroiwa K, Drobnjak M, Eastham J, et al. Clinically significant prostate cancer local recurrence after radiation therapy occurs at the site of primary tumor: magnetic resonance imaging and step-section pathology evidence. International journal of radiation oncology, biology, physics. 2007;69:62-9.

29. Cellini N, Morganti AG, Mattiucci GC, Valentini V, Leone M, Luzi S, et al. Analysis of intraprostatic failures in patients treated with hormonal therapy and radiotherapy: implications for conformal therapy planning. Int J Radiat Oncol Biol Phys. 2002;53:595-9.

30. Teste C, Schiavina R, Lodi R, et al. Prostate cancer: sextant localization with MR imaging, MR spectroscopy and 11C-choline PET/CT. Radiology 2007; 244: 797-806.

31. Mena E, Turkey B, Mani H, et al. 11C-Acetate PET/CT in localized prostate cancer: a study with MRI and histopathologic correlation. J Nucl Med 2012; 53: 538-545.

32. Fütterer J, Heijmink S, Schennen T, et al. Prostate cancer localization with dynamic contrast-enhanced MR imaging and proton MR spectroscopic imaging. Radiology 2006; 241: 449-458.

33. Groendael G, Borren A, Moman M, et al. Pathologic validation of a model based on diffusion-weighted imaging and dynamic contrast-enhanced magnetic resonance imaging for tumor delineation in the prostate peripheral zone. Int J Radiat Oncol Biol Phys 2012; 82: 537-544.

34. Lips IM, van der Heide UA, Haustermans K, et al. Single blind randomized phase III trial to investigate the benefit of a focal lesion ablative microboost in prostate cancer (FLAME-trial): study protocol for a randomized controlled trial. Trials. 2011;12:255.
35. Greer P, Dowling J, Lambert J, et al. A magnetic resonance imaging-based workflow for planning radiation therapy for prostate cancer. AMJ 2011; 194: S24-S27.

Table 1. Overview of the recommendations for the delineation of the rectum and clinical target volume of the prostate and seminal vesicles. Abbreviations: MRI: magnetic resonance imaging; CT scan: computed tomography scan; ECE: extracapsular extension.

Risk stratification:

low risk (PSA ≤10 ng/ml; biopsy Gleason score ≤6 and clinical stage ≤T2a and <50% of the biopsies involved

intermediate risk (PSA>10 and ≤20 ng/ml or Gleason score of 7 or clinical stage T2b)

high risk (PSA >20 ng/ml or Gleason score ≥8 or clinical stage ≥T2c)

Figure 1. Guide to delineate the rectum in the axial (figure A-C) and sagital (figure D) plane. In yellow the rectum contour is presented. The rectum is contoured were visible on axial planes (A-C). Then these rectum slices are projected in the sagital plane (yellow lines in figure D). These lines are subsequently connected to define the rectum and controlled in the sagital plane (figure D). Thereafter the delineated rectum in the sagital plane can again be visualised in the axial plane. The lines that are formed as such depict the anterior and posterior border of the rectum.

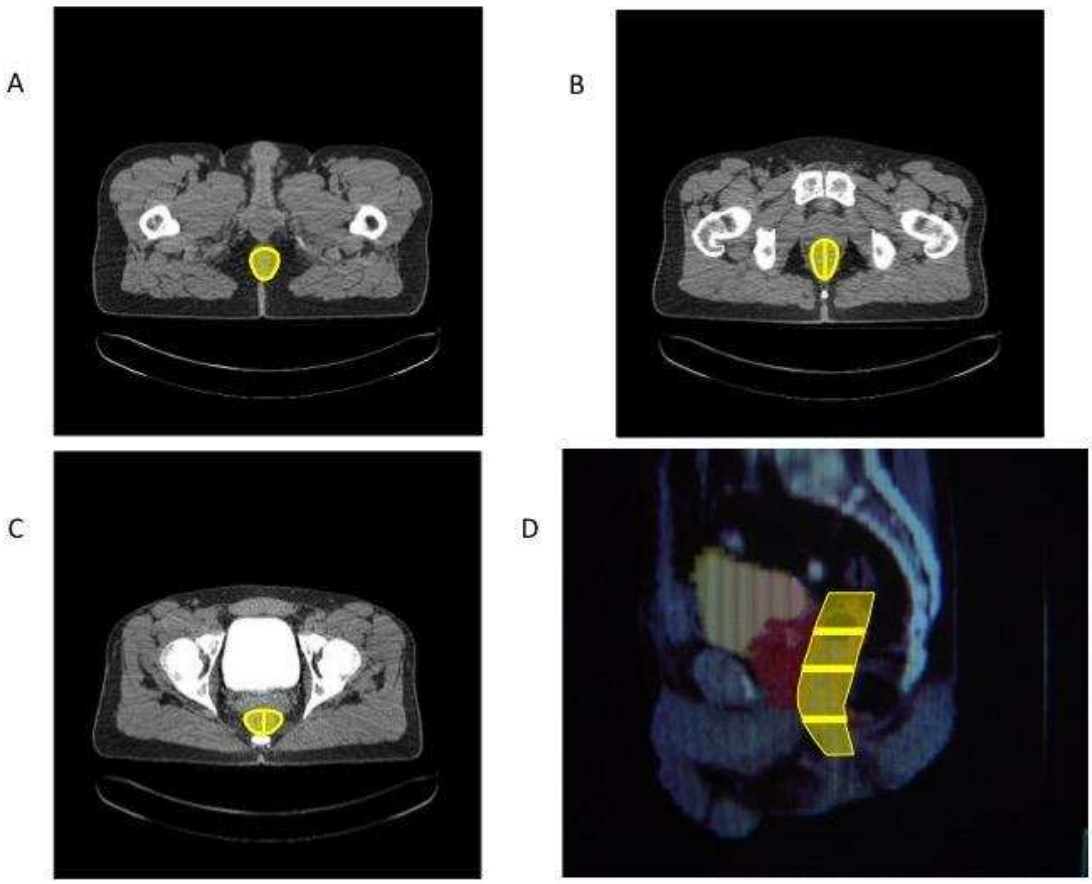

Figure 2. Delineation of the different parts of the prostate on CT scan and MRI. In red: deineation of the prostate on CT. The rectum is presented in yellow.

Figure 2a: penile bulb presented in blue.

Figure 2b: genito-urinary diaphragm.

Figure 2c: apex of the prostate on CT. The green lines represent the thickness of the levator ani muscles on CT extrapolated from the rectum part to the more anterior part. In pink the prostate contour as defined on MRI is presented demonstrating that the thickness of the levator ani muscles is larger on CT based delineation when compared to MRI based prostate contouring.

Figure 2D: Superposition of the MRI information at the level of the apex.

Figure 2E: Prostate contour at the level of the mid-prostate. The green lines again represent the thickness of the levator ani muscles on CT.

Figure 2F: Prostate contour at the level of the mid-prostate.

Figure 2G: Prostate contour at the level of the mid-prostate focusing on the anterior border. In pink the prostate cantour as defined on MRI is superimposed to the CT images.

Figure 2H: Superposition of the MRI information at the level of the mid prostate. In red the plexus of Santorini is illustrated.

Figure 2I: Prostate contour at the level of the base. By using contrast the bladder is clearly demarquated from the prostate contour.

Figure 2J: Contour of the seminal vesicles excluding the ejaculatory ducts located medialy of the seminal vesicles.

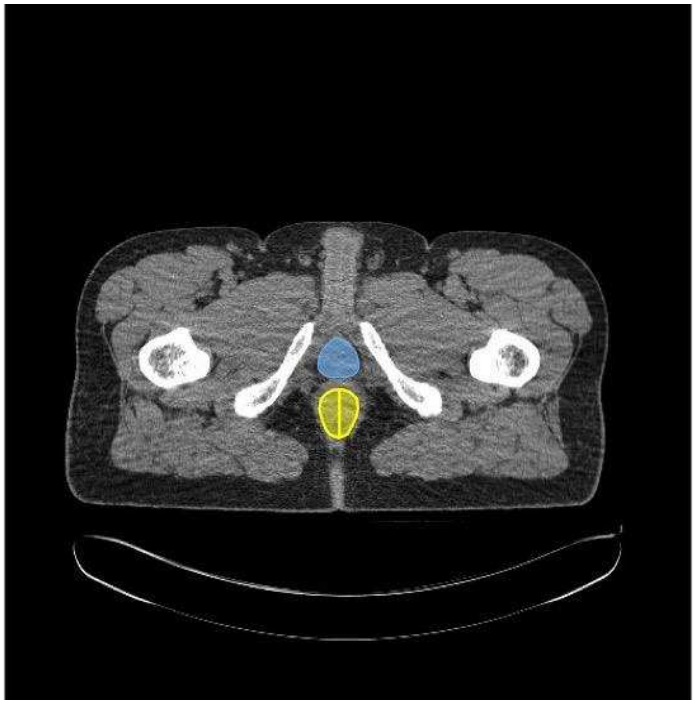

Figure 2A

Figure 2B

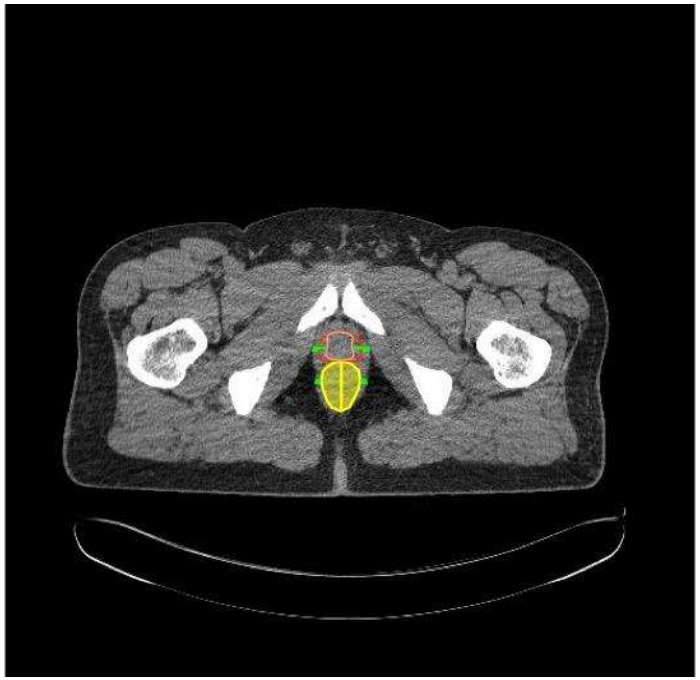

Figure 2C

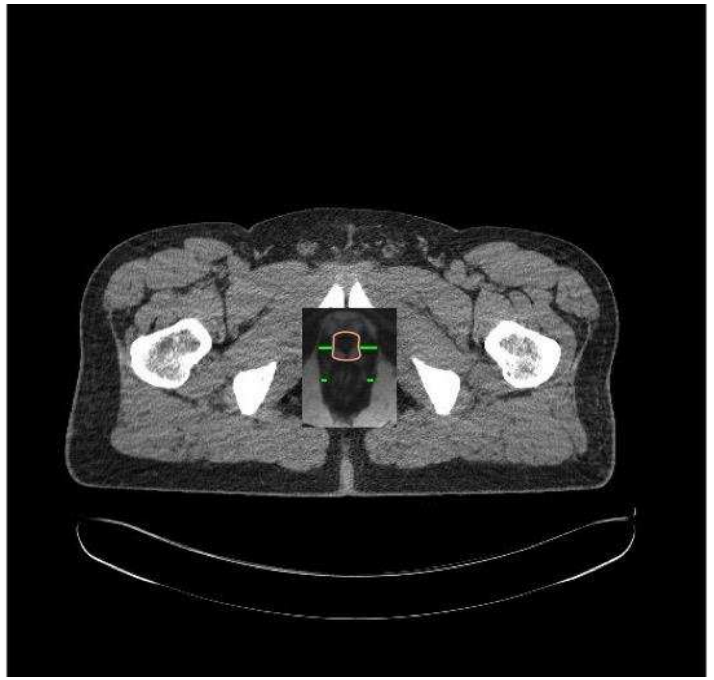

Figure 2D

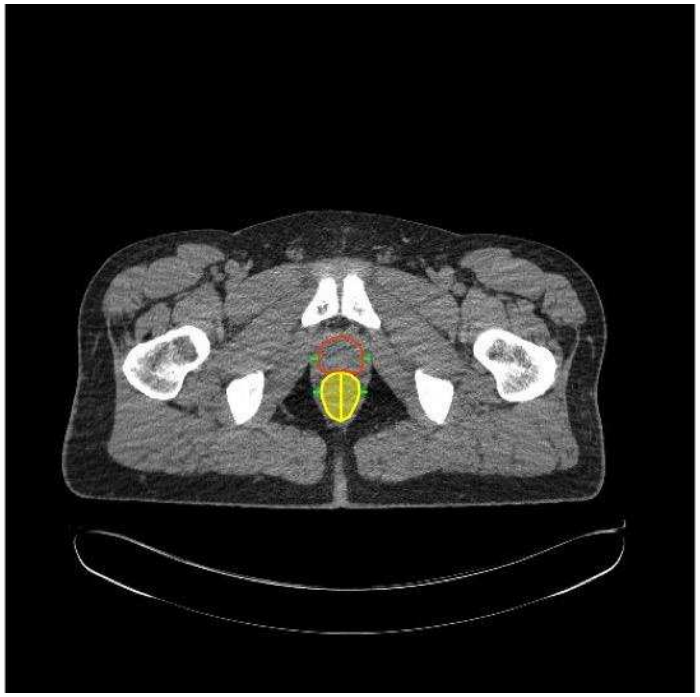

Figure 2E

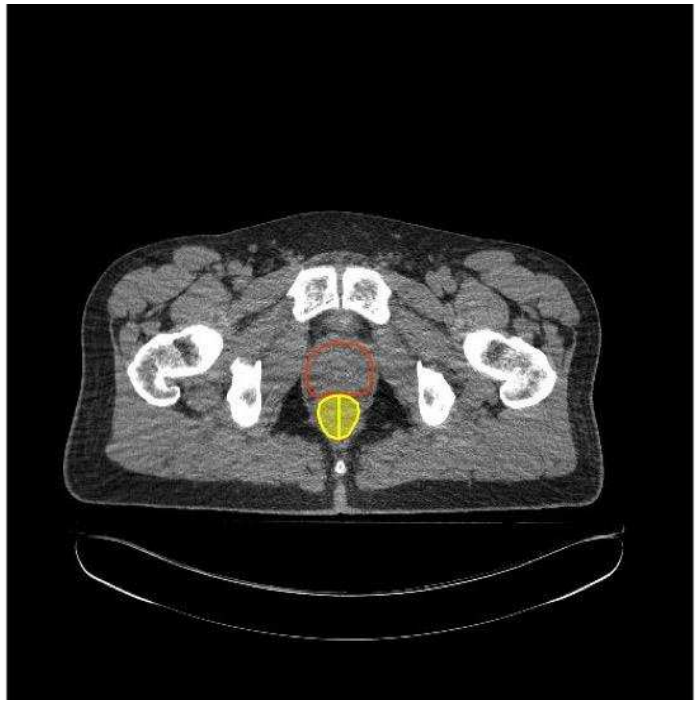

Figure 2F

Figure 2G

Figure 2H

Figure 2I

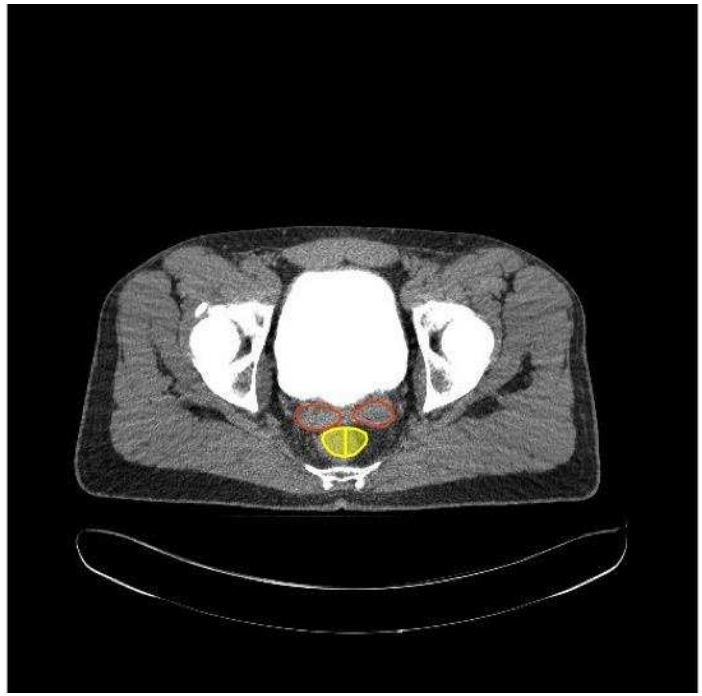

Figure 2J